

## Cycloaddition Reactions of Acrylonitrile on the Si(100)-2×1 Surface

Cheol Ho Choi\*<sup>†</sup> and Mark S. Gordon\*<sup>‡</sup>

Contribution from the Department of Chemistry, College of Natural Sciences, Kyungpook National University, Taegu 702-701, South Korea, and Ames Laboratory and Department of Chemistry, Iowa State University, Ames Iowa 50011

Received January 28, 2002

**Abstract:** Multi-reference as well as single-reference quantum mechanical methods were adopted to study the potential energy surface along three possible surface reaction mechanisms of acrylonitrile on the Si(100)-2×1 surface. All three reactions occur via stepwise radical mechanisms. According to the computed potential energy surfaces, both [4+2] and [2+2]<sub>CN</sub> cycloaddition products resulting from the reactions of surface dimers with the C≡N of acrylonitrile are expected, due to the negligible activation barriers at the surface. Another possible surface product, [2+2]<sub>CC</sub>, requires a 16.7 kcal/mol activation energy barrier. The large barrier makes this route much less favorable kinetically, even though this route produces the thermodynamically most stable products. Isomerization reactions among the surface products are very unlikely due to the predicted large activation barriers preventing thermal redistributions of the surface products. As a result, the distribution of the final surface products is kinetically controlled leading to a reinterpretation of recent experiments. An intermediate Lewis acid–base type complex appears in both the [4+2] and [2+2]<sub>CN</sub> cycloadditions entrance channels, indicating that the surface may act as an electrophile/Lewis acid toward a strong Lewis base substrate.

### I. Introduction

With the advances of new experimental techniques and the development of increasingly sophisticated quantum mechanical methods and computational hardware, increasing effort is being expended to develop synthetically modified semiconductor surfaces. Among the goals in these endeavors are the pursuit of enhanced properties for microelectronics, sensors, biologically active surfaces, and nonlinear optical materials.<sup>1</sup> Many saturated and unsaturated organic and organometallic compounds are actively being tested for the creation of new interfacial chemical bonds that would potentially add new functionalities to the semiconductor technology.

Surface reactions of unsaturated organic compounds with the Si(100)-2×1 reconstructed surface have attracted particular interest. Surface reactions of alkynes and alkenes with the Si(100)-2×1 surface are examples of [2<sub>s</sub>+2<sub>s</sub>] cycloadditions, which are formally orbital symmetry forbidden.<sup>2</sup> Thus, a large reaction barrier is expected along the symmetric reaction pathway. In fact, it is known from carbon solution chemistry that even the low-symmetry reaction pathway has a high reaction barrier, mainly due to unfavorable geometric configurations along the reaction path.<sup>3</sup> However, the rules governing [2+2]

additions on surfaces are apparently different, since many instances of formally forbidden reactions have been reported. Early experimental<sup>4</sup> and theoretical<sup>5</sup> studies have shown that ethylene, propylene, and acetylene easily chemisorb on Si(100)-2×1 yielding [2+2] products and are able to resist temperatures of up to 600 K.

Theoretically, Liu and Hoffmann<sup>5b</sup> have found a low-symmetry pathway that contains a  $\pi$ -complex precursor and a biradical intermediate that has a low energy barrier to [2+2] cycloaddition products, substantiating the experimental findings. Recent experimental<sup>6</sup> and theoretical<sup>7</sup> studies identified other possible surface products of acetylene, adding a new complexity to the surface reactions of ene systems.

Diene systems have also been actively studied. In the case of 1,3-butadiene and 2,3-dimethyl-1,3-butadiene, theoretical and experimental studies have shown<sup>8</sup> that the surface dimer can act as a good dienophile, yielding “Diels–Alder” or [4+2]-

- (3) Fleming, I. *Frontier Orbitals and Organic Chemical Reactions*; Wiley: New York, 1976; p 90.
- (4) (a) Nishijima, M.; Yoshinobu, J.; Tsuda, H.; Onchi, M. *Surf. Sci.* **1987**, *192*, 383. (b) Yoshinobu, J.; Tsuda, H.; Onchi, M.; Nishijima, M. *J. Chem. Phys.* **1987**, *87*, 7332. (c) Taylor, P. A.; Wallace, R. M.; Cheng, C. C.; Weinberg, W. H.; Dresser, M. J.; Choyke, W. J.; Yates, J. T., Jr. *J. Am. Chem. Soc.* **1992**, *114*, 6754. (d) Li, L.; Tindall, C.; Takaoka, O.; Hasegawa, Y.; Sakurai, T. *Phys. Rev. B* **1997**, *56*, 4648.
- (5) (a) Imamura, Y.; Morikawa, Y.; Yamasaki, T.; Nakasuji, H. *Surf. Sci.* **1995**, *341*, L1091. (b) Liu, Q.; Hoffmann, R. *J. Am. Chem. Soc.* **1995**, *117*, 4082.
- (6) (a) Wolkow, R. A. *Annu. Rev. Phys. Chem.* **1995**, *50*, 413. (b) Mezhenny, S.; Lyubinetzky, L.; Choyke, W. J.; Wolkow, R. A.; Yates, J. T., Jr. *Phys. Rev. Lett.*
- (7) Sorescu, D. C.; Jordan, K. D. *J. Phys. Chem. A* **2000**, *104*, 8259.
- (8) (a) Konecny, R.; Doren, D. *J. Am. Chem. Soc.* **1997**, *119*, 11098. (b) Teplyakov, A. V.; Kong, M. J.; Bent, S. F. *J. Am. Chem. Soc.* **1997**, *119*, 11100. (c) Teplyakov, A. V.; Kong, M. J.; Bent, S. F. **1998**, *108*, 4599.

\* Corresponding author. E-mail: cchoi@knu.ac.kr; mark@si.fi.ameslab.gov.

<sup>†</sup> Kyungpook National University.

<sup>‡</sup> Iowa State University.

- (1) (a) Buriak, J. M. *J. Chem. Soc., Chem. Commun.* **1995**, *95*, 1589. (b) Yates, J. T., Jr. *Science* **1998**, *279*, 335. (c) Lopinski, G. P.; Moffatt, D.; Wayner, D. D. M.; Wolkow, R. A. *Nature* **1998**, *392*, 909.
- (2) Woodward, R. B.; Hoffmann, R. *The Conservation of Orbital Symmetry*; Verlag Chemie: Weinheim, Germany, 1970.

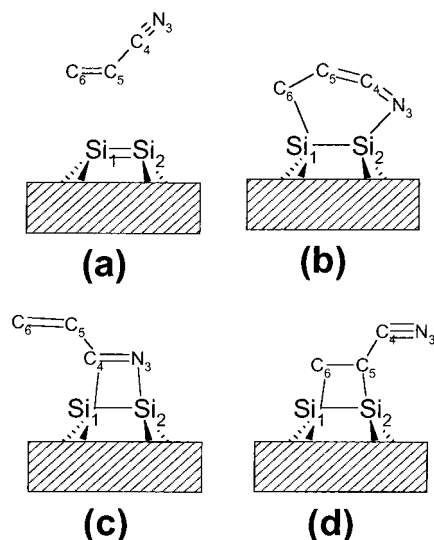


**Figure 1.** Reactants and three possible surface products: (a) the reactants; (b) the [4+2] product; (c) the [2+2]<sub>CN</sub> product; and (d) the [2+2]<sub>CC</sub> product.

cycloaddition products, in which a conjugated diene reacts with the silicon surface dimer to form a six-membered ring.

Reinvestigation of the 2,3-dimethyl-1,3-butadiene reaction on the Si(100)-2×1 surface by Hamers and co-workers<sup>9</sup> supported the observation that the Diels–Alder product represented 80% of the surface products. However, they noted a minor (20%) [2+2] product as well. In the case of 1,3-cyclohexadiene, they observed 55% of the [4+2] products, 35% of [2+2] product, and 10% unknown, strongly indicating the existence of competition between [4+2] and [2+2] reactions of the diene on the Si(100) surface. Attempts to convert the product distribution to the thermodynamically more stable product by annealing to higher temperatures failed. Subsequent theoretical studies<sup>10</sup> provided further support for the existence of the competing reactions by showing that there exists a low-energy [2+2] cycloaddition pathway on the Si(100) surface, and that the surface isomerization reaction connecting [4+2] and [2+2] products is very unlikely due to a high activation barrier.

These new experimental and theoretical studies indicate that the final surface reaction products are determined during the initial stage of the surface reactions, and that they are not subject to further thermal redistributions or isomerizations among surface products. This provides very strong evidence that the control of the surface selectivity toward a diene is determined by the reaction kinetics rather than the thermodynamics.

In this regard, the surface reactions of acrylonitrile, which has both a C≡N bond and a C=C bond, with the Si(100)-2×1 surface is of interest. It has been established<sup>11</sup> that the C=C bond of acrylonitrile acts as a dienophile with the electron-withdrawing CN group in traditional solution chemistry. However, it is possible that, on the Si(100)-2×1 surface, acrylonitrile may behave differently, since there is no diene to react with.

Three possible relatively stable reaction products are presented in Figure 1, where (a) represents the reactants, (b) represents

the [4+2] type product, in which Si<sub>1</sub>–C<sub>6</sub> and Si<sub>2</sub>–N<sub>3</sub> bonds are formed making an allenic N<sub>3</sub>=C<sub>4</sub>=C<sub>5</sub> configuration, (c) represents the [2+2]<sub>CN</sub> product with the formation of Si<sub>1</sub>–C<sub>4</sub> and Si<sub>2</sub>–N<sub>3</sub> bonds, and (d) represents the [2+2]<sub>CC</sub> product with Si<sub>1</sub>–C<sub>6</sub> and Si<sub>2</sub>–C<sub>5</sub> bonds being formed. Recent experiments by Tao et al.<sup>12</sup> suggest that acrylonitrile reacts only through the C≡N bond with Si dimers via a [2+2] cycloaddition mechanism, yielding exclusively the [2+2]<sub>CN</sub> surface product. This conclusion is in contrast to the surface reactions of the homonuclear conjugated diene systems as considered earlier, for which both [2+2] and [4+2] products were observed.

The question regarding whether and why only one of the many possible products is exclusively formed ultimately bears on the chemical selectivity of the Si(100)-2×1 surface toward conjugated diene systems, homonuclear and heteronuclear alike. By studying the factors that govern the reactivity of these species, one hopes to gain control over these surface reactions to an extent that eventually leads to a technique to tailor the reaction selectivity. In this paper, an extensive theoretical study of the potential energy surface of the reaction mechanisms is performed to elucidate the nature and origin of the Si(100)-2×1 surface selectivity toward acrylonitrile, a heteronuclear diene.

## II. Computational Details

Two basis sets were used in this work. The SBKJC effective core potential (ECP) and basis set<sup>13</sup> are used, augmented by *d* polarization functions<sup>14</sup> on all heavy atoms. This is referred to as SBK(d). To study basis set effects, a mixed basis set, referred to as MIXED, comprised of SBK(d) for Si and 6-31G(d) for C and N, was tested. In addition, the all-electron 6-31G(d)<sup>15</sup> basis set was also used. The minimum energy reaction paths were determined by first optimizing the geometries of the minima and transition states. Then, each stationary point was characterized by computing and diagonalizing the Hessian matrix (matrix of energy second derivatives). To follow the minimum energy path (MEP), the Gonzalez-Schlegel second-order method<sup>16</sup> was used with a step size of 0.3 amu<sup>1/2</sup>·bohr.

Various points on the reaction paths, particularly transition states and intermediates, are often inherently multi-configurational. Therefore CASSCF (complete active space SCF)<sup>17</sup> wave functions were primarily used to describe these species. The selected orbitals for the active space are now discussed in detail. For the study of the reaction paths leading to the products [4+2] and [2+2]<sub>CN</sub>, an (8,8) active space was used. This active space is constructed from the 6 electrons in the three sets of  $\pi$  and  $\pi^*$  orbitals of acrylonitrile, plus the 2 electrons and  $\pi$  and  $\pi^*$  orbitals of the surface Si dimer. For the study of the reaction path leading to the product [2+2]<sub>CC</sub>, a (6,6) active space is used consisting of the 2 electrons and the  $\pi$  and  $\pi^*$  orbitals of the acrylonitrile C=C bond, plus the 4 electrons associated with the  $\pi$ ,  $\pi^*$ ,  $\sigma$ , and  $\sigma^*$  orbitals of the surface Si dimer. A smaller active space is chosen in this case,

- (12) Tao, F.; Sim, W. S.; Xu, G. Q.; Qiao, M. H. *J. Am. Chem. Soc.* **2001**, *123*, 9397–9403.  
 (13) (a) Stevens, W. J.; Basch, H.; Krauss, M. *J. Chem. Phys.* **1984**, *81*, 6026. (b) Stevens, W. J.; Krauss, M.; Basch, H.; Jasien, P. G. *Can. J. Chem.* **1992**, *70*, 612. (c) Cundari, T. R.; Stevens, W. J. *J. Chem. Phys.* **1993**, *98*, 5555.  
 (14) Hariharan, P. C.; Pople, J. A. *Theor. Chim. Acta* **1973**, *28*, 213.  
 (15) Hehre, W. J.; Ditchfield, R.; Pople, J. A. *J. Chem. Phys.* **1972**, *56*, 2257.  
 (16) (a) Gonzalez, C.; Schlegel, H. B. *J. Phys. Chem.* **1990**, *94*, 5523. (b) Gonzalez, C.; Schlegel, H. B. *J. Chem. Phys.* **1991**, *95*, 5853.  
 (17) (a) Sunberg, K. R.; Ruedenberg, K. In *Quantum Science*; Calais, J. L., Goscinski, O., Linderberg, J., Ohm, Y., Eds.; Plenum: New York, 1976. (b) Cheung, L. M.; Sunberg, K. R.; Ruedenberg, K. *Int. J. Quantum Chem.* **1979**, *16*, 1103. (c) Ruedenberg, K.; Schmidt, M.; Gilbert, M. M.; Elbert, S. T. *Chem. Phys.* **1982**, *71*, 41. (d) Roos, B. O.; Taylor, P.; Siegbahn, P. E. *Chem. Phys.* **1980**, *48*, 157. (e) Schmidt, M. W.; Gordon, M. S. *Annu. Rev. Phys. Chem.* **1998**, *49*, 233.

- (9) Hovis, J. S.; Liu, H. B.; Hamers, R. J. *J. Phys. Chem. B* **1998**, *102*, 6873.  
 (10) (a) Choi, C. H.; Gordon, M. S. *J. Am. Chem. Soc.* **1999**, *121*, 11311. (b) Choi, C. H.; Gordon, M. S. In *The Chemistry of Organic Silicon Compounds*; Rappoport, Z., Apeloig, Y., Eds.; John Wiley & Sons: New York, 2001; Vol. 3, Chapter 15, pp 821–852.  
 (11) Fleming, I. *Frontier Orbitals and Organic Chemical Reactions*; Wiley: London, 1976.

**Table 1.** Geometric Data (Å) and MRMP2 Energetics (kcal/mol) of the Products, Intermediates, and Transition States

	bond lengths						$\Delta E^a$
<b>1b</b> , [4+2]	2.411 (Si <sub>1</sub> –Si <sub>2</sub> )	1.852 (Si <sub>2</sub> –N <sub>3</sub> )	1.234 (N <sub>3</sub> –C <sub>4</sub> )	1.328 (C <sub>4</sub> –C <sub>5</sub> )	1.527 (C <sub>5</sub> –C <sub>6</sub> )	1.982 (Si <sub>1</sub> –C <sub>6</sub> )	9.8 (19.4) <sup>b</sup>
<b>1c</b> , [2+2] <sub>CN</sub>	2.331 (Si <sub>1</sub> –Si <sub>2</sub> )	1.853 (Si <sub>2</sub> –N <sub>3</sub> )	1.295 (N <sub>3</sub> –C <sub>4</sub> )	1.471 (C <sub>4</sub> –C <sub>5</sub> )	1.343 (C <sub>5</sub> –C <sub>6</sub> )	1.999 (Si <sub>1</sub> –C <sub>6</sub> )	14.2 (21.5) <sup>b</sup>
<b>1d</b> , [2+2] <sub>CC</sub>	2.347 (Si <sub>1</sub> –Si <sub>2</sub> )	2.000 (Si <sub>2</sub> –C <sub>5</sub> )	1.160 (N <sub>3</sub> –C <sub>4</sub> )	1.466 (C <sub>4</sub> –C <sub>5</sub> )	1.567 (C <sub>5</sub> –C <sub>6</sub> )	1.983 (Si <sub>1</sub> –C <sub>6</sub> )	0.0 (0.0) <sup>b</sup>
<b>3a</b> , I <sub>[4+2]</sub> –[2+2] <sub>CN</sub>	2.400 (Si <sub>1</sub> –Si <sub>2</sub> )	1.965 (Si <sub>2</sub> –N <sub>3</sub> )	1.151 (N <sub>3</sub> –C <sub>4</sub> )	1.442 (C <sub>4</sub> –C <sub>5</sub> )	1.342 (C <sub>5</sub> –C <sub>6</sub> )		–30.4 (–30.8) <sup>c</sup>
<b>3b</b> , TS <sub>[4+2]</sub>	2.341 (Si <sub>1</sub> –Si <sub>2</sub> )	2.086 (Si <sub>2</sub> –N <sub>3</sub> )	1.184 (N <sub>3</sub> –C <sub>4</sub> )	1.387 (C <sub>4</sub> –C <sub>5</sub> )	1.381 (C <sub>5</sub> –C <sub>6</sub> )	2.916 (Si <sub>1</sub> –C <sub>6</sub> )	–4.3 (–1.8) <sup>c</sup>
<b>3c</b> , TS <sub>[2+2]<sub>CN</sub></sub>	2.395 (Si <sub>1</sub> –Si <sub>2</sub> )	1.866 (Si <sub>2</sub> –N <sub>3</sub> )	1.193 (N <sub>3</sub> –C <sub>4</sub> )	1.451 (C <sub>4</sub> –C <sub>5</sub> )	1.339 (C <sub>5</sub> –C <sub>6</sub> )	2.849 (Si <sub>1</sub> –C <sub>4</sub> )	3.3 (23.9) <sup>c</sup>
<b>3d</b> , TS <sub>I<sub>[2+2]<sub>CC</sub></sub></sub>	2.643 (Si <sub>1</sub> –Si <sub>2</sub> )	2.374 (Si <sub>1</sub> –C <sub>6</sub> )	1.391 (C <sub>5</sub> –C <sub>6</sub> )	2.199 (Si <sub>1</sub> –C <sub>5</sub> )	3.605 (Si <sub>2</sub> –C <sub>5</sub> )		4.0 (16.5) <sup>c</sup>
<b>3e</b> , I <sub>[2+2]<sub>CC</sub></sub>	4.379 (Si <sub>1</sub> –Si <sub>2</sub> )	1.904 (Si <sub>1</sub> –C <sub>6</sub> )	1.535 (C <sub>5</sub> –C <sub>6</sub> )	1.943 (Si <sub>1</sub> –C <sub>5</sub> )	4.067 (Si <sub>2</sub> –C <sub>5</sub> )		13.3 (28.9) <sup>c</sup>
<b>3f</b> , TS <sub>2<sub>[2+2]<sub>CC</sub></sub></sub>	3.057 (Si <sub>1</sub> –Si <sub>2</sub> )	1.885 (Si <sub>1</sub> –C <sub>6</sub> )	1.531 (C <sub>5</sub> –C <sub>6</sub> )	2.263 (Si <sub>1</sub> –C <sub>5</sub> )	2.523 (Si <sub>2</sub> –C <sub>5</sub> )		13.1 (8.5) <sup>c</sup>
<b>3g</b>	2.370 (Si <sub>1</sub> –Si <sub>2</sub> )	2.364 (Si <sub>2</sub> –N <sub>3</sub> )	2.177 (Si <sub>2</sub> –C <sub>4</sub> )	2.465 (Si <sub>2</sub> –C <sub>5</sub> )	1.967 (Si <sub>1</sub> –C <sub>6</sub> )		16.7 (28.6) <sup>c</sup>
<b>3h</b>	2.430 (Si <sub>1</sub> –Si <sub>2</sub> )	2.870 (Si <sub>1</sub> –C <sub>4</sub> )	1.981 (Si <sub>1</sub> –C <sub>5</sub> )	2.290 (Si <sub>1</sub> –C <sub>6</sub> )	1.790 (Si <sub>2</sub> –N <sub>3</sub> )		37.6 (43.0) <sup>d</sup>
							42.4 (58.1) <sup>d</sup>

<sup>a</sup> Values in parentheses are CASSCF(8,8)/MIXED energies, except **3d**, **3e**, and **3f** energies are obtained with CASSCF(6,6)/MIXED theory. <sup>b</sup> Values represent the relative energies with respect to **1d**. <sup>c</sup> Values are energies relative to separated reactants (acrylonitrile + bare silicon surface). <sup>d</sup> Energies relative to **1b** product.

since the CN group does not participate in this part of the reaction surface. Inclusion of the silicon surface dimer  $\sigma$  bond is necessary, since it is broken during the reaction. For the study of the surface isomerization reactions, the larger (8,8) active space is used.

To recover the dynamic electron correlation, and to ensure that all parts of the reaction path are treated equivalently, multi-reference second-order perturbation theory was used, since the level of accuracy for such methods is at least comparable to that of MP2 when single reference methods are appropriate.<sup>18</sup> The particular version of this method used in the present work is referred to as MRMP2 (multi-reference second-order perturbation theory).<sup>19</sup> For comparison with the results of these multi-reference calculations, calculations have also been performed with three single-reference methods: Hartree–Fock (HF), density functional theory (DFT) with the B3LYP<sup>20</sup> exchange–correlation functional, and second-order Møller–Plesset perturbation theory (MP2).<sup>21</sup> The GAMESS (General atomic and molecular electronic structure system)<sup>22</sup> program was used for all of the computations.

The all-quantum mechanics (QM) calculations were performed using the Si<sub>9</sub>H<sub>12</sub> silicon cluster model shown in Figure 2a. To study the surface size effect, a hybrid quantum mechanics/molecular mechanics (QM/MM) method called SIMOMM<sup>23</sup> (surface integrated molecular orbital molecular mechanics) was used. The SIMOMM cluster is composed of a C<sub>3</sub>NSi<sub>9</sub>H<sub>15</sub> quantum region embedded in a C<sub>3</sub>NSi<sub>48</sub>H<sub>52</sub> cluster. MM3<sup>24</sup> parameters were used for the molecular mechanics optimization part of the computations. Figure 2b illustrates the SIMOMM model, where the quantum mechanical Si atoms are in purple. All of the computations were done without imposing symmetry unless otherwise specified.

### III. Results and Discussions

**A. Surface Products.** Fully optimized geometric parameters and relative energetics of the most likely surface products were calculated with various methods. Only the CASSCF and

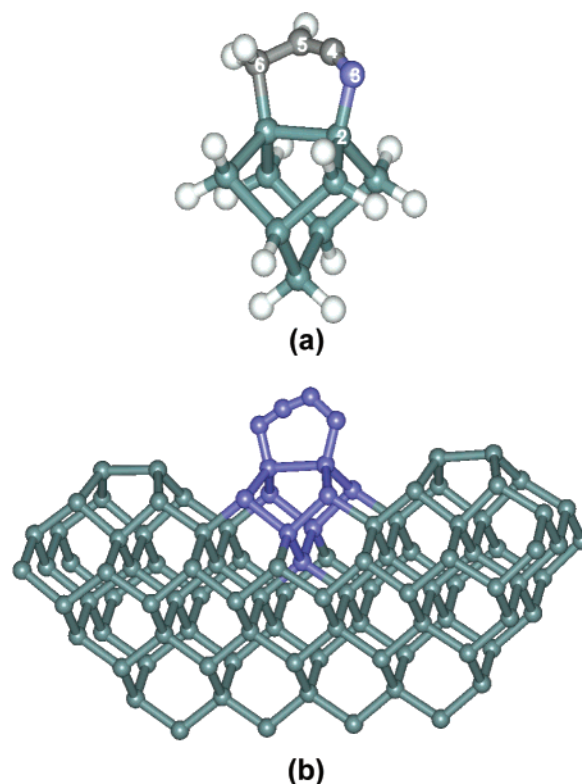


**Figure 2.** (a) The C<sub>3</sub>NSi<sub>9</sub>H<sub>15</sub> quantum model and (b) the SIMOMM model composed of a C<sub>3</sub>NSi<sub>9</sub>H<sub>15</sub> quantum region embedded in a C<sub>3</sub>NSi<sub>48</sub>H<sub>52</sub> cluster. The quantum mechanical atoms are in purple.

MRMP2 results are presented in Table 1. More extensive data can be found in the Supporting Information.

In the table, energies of [4+2] and [2+2]<sub>CN</sub> products are given relative to that of [2+2]<sub>CC</sub>. Bond lengths obtained using the various methods are all in reasonable agreement with each other (see Supporting Information). In particular, the geometric parameters obtained with the SIMOMM method are consistent with those predicted by the full ab initio models, indicating that the 9-silicon model may describe the actual experimental system reasonably well.

With regard to relative energies, most methods and basis sets are in good agreement with each other, but B3LYP consistently underestimates the stabilities of [2+2]<sub>CC</sub> with respect to [4+2] and [2+2]<sub>CN</sub> by 7–8 kcal/mol compared with the other methods (see Supporting Information). The relative energies obtained with the SIMOMM model, which includes a larger surface

- (18) (a) Werner, H.-J. *Mol. Phys.* **1996**, *89*, 645. (b) Schmidt, M. S.; Gordon, M. S. *Ann. Rev. Phys. Chem.* **1998**, *49*, 233. (c) Glaesemann, K. R.; Gordon, M. S.; Nakano, H. *PCCP* **1999**, *1*, 967.
- (19) (a) Nakano, H. *J. Chem. Phys.* **1993**, *99*, 7983. (b) Nakano, H. *Chem. Phys. Lett.* **1993**, *207*, 372.
- (20) (a) Becke, A. D. *J. Chem. Phys.* **1993**, *98*, 5648. (b) Stephens, P. J.; Devlin, F. J.; Chablowski, C. F.; Frisch, M. J. *J. Phys. Chem.* **1994**, *98*, 11623. (c) Hertwig, R. H.; Koch, W. *Chem. Phys. Lett.* **1997**, *268*, 345–351.
- (21) Møller, C.; Plesset, M. S. *Phys. Rev.* **1934**, *46*, 618.
- (22) (a) Schmidt, M. W.; Baldrige, K. K.; Boatz, J. A.; Elbert, S. T.; Gordon, M. S.; Jensen, J. H.; Koseki, S.; Matsunaga, N.; Nguyen, K. A.; Su, S.; Windus, T. L.; Dupuis, M.; Montgomery, J. A., Jr. *J. Comput. Chem.* **1993**, *14*, 1347. (b) Fletcher, G. D.; Schmidt, M. W.; Gordon, M. S. *Adv. Chem. Phys.* **1999**, *110*, 267.
- (23) Shoemaker, J. R.; Burgraff, L. W.; Gordon, M. S. *J. Phys. Chem. A* **1999**, *103*, 3245.
- (24) (a) Allinger, N. L.; Yuh, Y. H.; Lii, J. H. *J. Am. Chem. Soc.* **1989**, *111*, 8551. (b) Lii, J. H.; N. L. Allinger, *J. Am. Chem. Soc.* **1989**, *111*, 8566. (c) Lii, J. H.; N. L. Allinger, *J. Am. Chem. Soc.* **1989**, *111*, 8576.

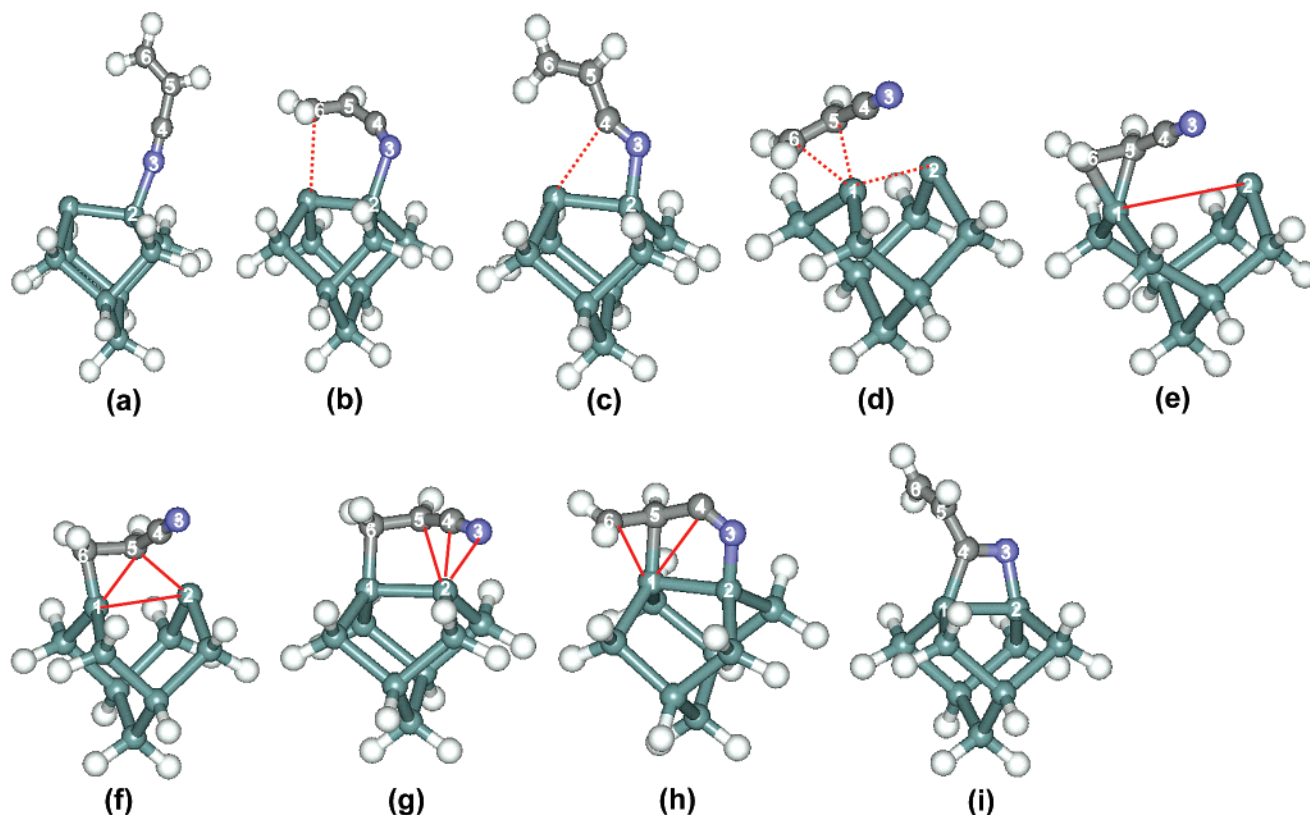


**Figure 3.** Intermediates and transition states along the surface reactions: (a)  $I_{[4+2]-[2+2]CN}$ , an intermediate where N donates lone pair electrons to the surface; (b)  $TS_{[4+2]}$ , a transition state that connects (a) and [4+2]; (c)  $TS_{[2+2]CN}$ , a transition state that connects (a) and [2+2]<sub>CN</sub>; (d)  $TS_{I[2+2]CC}$ , a transition state that connects the reference point and (e); (e)  $I_{[2+2]CC}$ , an intermediate along the [2+2]<sub>CC</sub> product mechanism; (f)  $TS_{[2+2]CC}$ , a transition state that connects (e) and [2+2]<sub>CC</sub>; (g)  $TS_{[4+2] \leftrightarrow [2+2]CC}$ , a transition state that connects [4+2] and [2+2]<sub>CC</sub>; (h)  $TS_{[4+2] \leftrightarrow [2+2]CN}$ , a transition state that connects [4+2] and [2+2]<sub>CN</sub>; and (i)  $I_R$ , a transition state of the surface internal rotation.

effect, agree with the corresponding fully QM results to within 1–2 kcal/mol. All calculations predict that [2+2]<sub>CC</sub> is the most stable surface product followed by [4+2] and [2+2]<sub>CN</sub> with relative MRMP2/MIXED energies for the latter two of 9.8 and 14.2 kcal/mol, respectively. The remaining discussion will focus on this level of theory.

There is not an obvious rationale for the relative stabilities of [4+2] and [2+2]<sub>CN</sub>. Although [4+2] has a less strained six-membered ring, it also has a destabilizing allenic moiety. In contrast, [2+2]<sub>CN</sub> has a strained four-membered ring. As a result of these competing factors, [4+2] is calculated to be more stable than [2+2]<sub>CN</sub> by about 5 kcal/mol. From a thermodynamic point of view, the [2+2]<sub>CC</sub> product would be the most likely to exist on the surface followed by [4+2] and [2+2]<sub>CN</sub>. Recent DFT-(B3LYP/6-31G(d) and PBP/DN\*\*) results reported by Tao et al.<sup>12</sup> predict [2+2]<sub>CN</sub> to be more stable than [4+2] by about 5 kcal/mol, in contrast to the results reported here. It is not clear why those authors' B3LYP/6-31G(d) results differ from those reported here.

The MRMP2(8,8)/MIXED energy of [2+2]<sub>CC</sub> with respect to the reactants (acrylonitrile + the bare surface), also presented in Table 1, is predicted to be -30.4 kcal/mol. In fact, all of the multi-reference methods predict the stability of this product to be in the 30–38 kcal/mol range. In contrast, all single reference methods overestimate the stability of this product. The CASSCF natural orbital occupation numbers (NOON) for the active space orbitals, a good measure of multi-configurational character, are 1.94, 1.94, 1.90, 1.66, 0.34, 0.10, 0.06, and 0.06 for the reactants, while those of [2+2]<sub>CC</sub> are 1.98, 1.98, 1.94, 1.94, 0.06, 0.06,

0.02, and 0.02. Clearly, reactants have stronger multi-configurational nature, primarily due to the significant diradical character of the surface Si dimer.<sup>25</sup> As a result, all single-configurational methods fail to predict the correct relative stabilities of products with respect to reactants. However, the relative stabilities among the products are predicted relatively well by most single-configurational methods, since the products are all less multi-configurational. It is also found that MRMP2-(8,8)/SBK(d) overestimates the stability of [2+2]<sub>CC</sub> by 7.8 kcal/mol as compared to MRMP2(8,8)/MIXED. This is consistent with previous results that suggest effective core potentials may be suspect for the lightest elements.<sup>26</sup>

As discussed in detail in an earlier study of the addition of 1,3-cyclohexadiene to the Si(100) surface,<sup>10</sup> the relative thermodynamic energies of the final products need not be correlated with the actual final product distribution, if the energetics are dominated by kinetic effects, i.e., the barrier heights of competing mechanisms. To determine whether the same is true for the system of interest here, the potential energy surfaces of the possible reaction mechanisms are studied and presented in the subsequent sections.

**B. Reaction Mechanism Leading to the [4+2] Product (1b).** The intermediate and transition state structures for the mechanism leading to the [4+2] product are presented in Figure 3. The corresponding fully optimized geometric data and relative

(25) (a) Redondo, A.; Goddard, W. A., III *J. Vac. Sci. Technol.* **1982**, *21*, 344. (b) Shoemaker, J.; Burggarf, L. W.; Gordon, M. S. *J. Chem. Phys.* **2000**, *112*, 2994.

(26) Jung, Y.; Choi, C. H.; Gordon, M. S. *J. Phys. Chem. B* **2001**, *105*, 4039.

energies are listed in Table 1. In analogy with the “Diels–Alder” reaction, one would expect a concerted reaction mechanism, in which both  $\text{Si}_1\text{--C}_6$  and  $\text{Si}_2\text{--N}_3$  bonds are forming at the same time. However, the initial surface product turns out to be the intermediate  $\text{I}_{[4+2]\text{--}[2+2]\text{CN}}$  (**3a**), which forms without any activation barrier. In this intermediate, only the  $\text{Si}_2\text{--N}_3$  bond has been formed. The reactivity of  $\text{N}_3$  with the surface dimer is apparently greater than that of  $\text{C}_4$ , perhaps because  $\text{N}_3$  has lone pair electrons. Therefore, even though the molecule might initially approach the surface in a concerted fashion, it eventually becomes  $\text{I}_{[4+2]\text{--}[2+2]\text{CN}}$ . So, the surface can act as an electrophile or a Lewis acid.

The MRMP2(8,8)/MIXED level of theory predicts a 4.3 kcal/mol stabilization energy for intermediate **3a**. As discussed in section A, single-configurational methods underestimate significantly the stabilities of reactants due to the lack of nondynamical electron correlation. As a result, single-configuration-based methods are not able to consistently provide accurate relative energies across the entire part of the potential energy surface of importance to the dissociation/adsorption reactions. The relatively small MRMP2 stabilization energy of  $\text{I}_{[4+2]\text{--}[2+2]\text{CN}}$  indicates that the bonding of  $\text{N}_3\text{--Si}_2$  is probably best described as a weak Lewis acid–base complex.

Transition state  $\text{TS}_{[4+2]}$  (**3b**), in which  $\text{C}_6$  is making a bond with  $\text{Si}_1$ , connects intermediate  $\text{I}_{[4+2]\text{--}[2+2]\text{CN}}$  with final product  $[4+2]$  (**1b**) with a forward activation energy of 7.6 kcal/mol relative to the intermediate and 3.3 kcal/mol relative to the initial reactants (Table 1). This small activation barrier suggests that the  $[4+2]$  products will be present on the surface.

**C. Reaction Mechanism Leading to the  $[2+2]_{\text{CN}}$  Product (**1c**).** Transition state  $\text{TS}_{[2+2]\text{CN}}$  (**3c**), in which  $\text{C}_4$  approaches  $\text{Si}_1$ , connects intermediate  $\text{I}_{[4+2]\text{--}[2+2]\text{CN}}$  with final product  $[2+2]_{\text{CN}}$  (**1c**) with a MRMP (8,8)/MIXED forward activation energy of 8.3 kcal/mol relative to the intermediate and 4.0 kcal/mol relative to the initial reactants. The latter is again rather small, so that the  $[2+2]_{\text{CN}}$  product is expected to be viable based on kinetic considerations. Note that the  $[4+2]$  and  $[2+2]_{\text{CN}}$  products both arise from the same initial intermediate state  $\text{I}_{[4+2]\text{--}[2+2]\text{CN}}$ . However, they go through different transition states,  $\text{TS}_{[4+2]}$  and  $\text{TS}_{[2+2]\text{CN}}$ , respectively.

Both channels require very small overall activation barriers, strongly suggesting the existence of both products, at least in the initial stages of adsorption processes.

**D. Reaction Mechanism Leading to the  $[2+2]_{\text{CC}}$  Product (**1d**).** To study this part of potential energy surface, the (6,6) active space discussed earlier was employed. Fully optimized geometric parameters and relative energies along the potential surface are listed in Table 1.

Transition state  $\text{TS}_{[2+2]\text{CC}}$  (**3d**) connects the separated reactants and the intermediate  $\text{I}_{[2+2]\text{CC}}$  (**3e**) with a MRMP2-(6,6)/MIXED forward activation barrier of 13.3 kcal/mol. In  $\text{TS}_{[2+2]\text{CC}}$ , both  $\text{C}_5$  and  $\text{C}_6$  interact with  $\text{Si}_1$  with a concomitant elongation of the  $\text{Si}_1\text{--Si}_2$  distance by about 0.2 Å from its original value. In the intermediate  $\text{I}_{[2+2]\text{CC}}$ , both  $\text{C}_5$  and  $\text{C}_6$  have formed bonds with  $\text{Si}_1$ , and the  $\text{Si}_1\text{--Si}_2$  distance is now  $>4$  Å, indicating that a diradical has been created.  $\text{I}_{[2+2]\text{CC}}$  is less stable than the reactants by 13.1 kcal/mol. So, this intermediate is barely more stable than the preceding transition state. From this point, only a small forward activation barrier of 3.6 kcal/mol at the transition state  $\text{TS}_{[2+2]\text{CC}}$  (**3f**) separates the intermediate

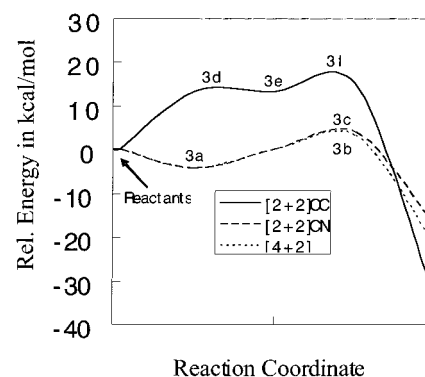


**Figure 4.** A schematic illustration of the reaction coordinates of the three competing surface mechanisms.

$\text{I}_{[2+2]\text{CC}}$  from the final product  $[2+2]_{\text{CC}}$ . In  $\text{TS}_{[2+2]\text{CC}}$  the  $\text{Si}_1\text{--C}_5$  bond is breaking and the new bonds  $\text{Si}_1\text{--Si}_2$  and  $\text{Si}_2\text{--C}_5$  are forming.

The overall reaction barrier to form the product  $[2+2]_{\text{CC}}$  is 16.7 kcal/mol. This is significantly larger than those separating the products  $[4+2]$  and  $[2+2]_{\text{CN}}$  from the reactants. This strongly suggests that the cycloaddition at the  $\text{C}=\text{C}$  center is kinetically less favorable than the two competing mechanisms. The overall reaction coordinates of the three competing mechanisms are comparatively illustrated in Figure 4. Since the actual experiment was done at the very low temperature of 110 K, the 16.7 kcal/mol barrier is likely to be a significant obstacle. It is possible that at high temperature, this channel can be activated.

In the previous calculation of the  $[2+2]$  cycloaddition of 1,3-cyclohexadiene to the  $\text{Si}(100)$  surface,<sup>10</sup> the overall reaction barrier was calculated to be about 5 kcal/mol. This is smaller than the analogous barrier obtained in this work. This difference may be due to the different substituents. In particular, in the current work, the strongly electron-withdrawing  $\text{C}\equiv\text{N}$  group would retard the reactions by removing electron density in the ene group making it less nucleophilic.

**E. Surface Isomerization Among Surface Products.** The initial surface products may undergo subsequent surface isomerization reactions. If these isomerizations occur with small barriers, the final product distribution may still be controlled by the product thermodynamics. It is therefore necessary to study the possible surface isomerization mechanisms. The relevant data are summarized in Table 1.

First, consider the isomerization between  $[4+2]$  (**1b**) and  $[2+2]_{\text{CC}}$  (**1d**). The transition state  $\text{TS}_{[4+2]\leftrightarrow[2+2]\text{CC}}$  (**3g**) is reached by breaking the  $\text{Si}_2\text{--N}_3$  bond and forming the  $\text{Si}_2\text{--C}_5$  bond. This transition state connects final products  $[4+2]$  and  $[2+2]_{\text{CC}}$  with a MRMP(8,8)/MIXED forward activation barrier of 37.6 kcal/mol.<sup>27</sup> Such a high barrier effectively prevents this isomerization channel, except at very high temperatures.

The transition state  $\text{TS}_{[4+2]\leftrightarrow[2+2]\text{CN}}$  (**3h**), which connects products  $[4+2]$  and  $[2+2]_{\text{CN}}$ , is obtained by breaking the  $\text{Si}_1\text{--C}_6$  bond and forming the  $\text{Si}_1\text{--C}_4$  bond. The forward activation energy associated with  $\text{TS}_{[4+2]\leftrightarrow[2+2]\text{CN}}$  is 42.4 kcal/mol. Therefore, one also expects that the isomerization reaction between  $[4+2]$  and  $[2+2]_{\text{CN}}$  is unlikely to occur, except at very high temperatures. These large barriers are both higher than those

(27) Note that MRMP2/MIXED calculations are not necessary in this part of the potential energy surface, since only the relative energies of the products are of interest, not energetics involving the diradicaloid reactants.

of the corresponding desorption barriers, so that desorption is more likely to occur than these isomerizations. There appears to be no direct path between the products  $[2+2]_{\text{CC}}$  and  $[2+2]_{\text{CN}}$  without going through product  $[4+2]$ .

In summary, even if sufficient thermal energy is provided to the surface products, surface isomerization would not occur among the possible surface products. This theoretical result is consistent with the experimental observations that the features related to chemisorbed species remain constant until around 450 K, above which desorption and decomposition occur.<sup>12</sup>

**F. Internal Rotation of the Surface Product 1b.** The C=C bond of the surface product  $[2+2]_{\text{CN}}$  can rotate internally through the C<sub>4</sub>–C<sub>5</sub> conjugated single bond via the transition state TS<sub>R</sub> (**3i**) with a B3LYP activation barrier of 8.2 kcal/mol. This internal rotation may be activated at high temperatures.

#### IV. Conclusions

Potential energy surface scans along possible reaction paths leading to the final products, and the isomerization reactions among them, were investigated with various quantum mechanical methods including multi-configurational second-order perturbation theory.

Thermodynamically,  $[2+2]_{\text{CC}}$  (**1d**) is the most stable surface product, followed by  $[4+2]$  (**1b**) and  $[2+2]_{\text{CN}}$  (**1b**). The latter are 9.8 and 14.2 kcal/mol higher in energy, respectively. However, the overall reaction barriers leading to  $[4+2]$ ,  $[2+2]_{\text{CN}}$ , and  $[2+2]_{\text{CC}}$  products are calculated to be 3.3, 4.0, and 16.7 kcal/mol, respectively, thereby making the  $[2+2]_{\text{CC}}$  product *kinetically* much less favorable. All three channels constitute stepwise radical mechanisms. Due to the high reactivity of the CN group, a concerted reaction mechanism leading to the  $[4+2]$  product does not exist. Instead, a Lewis acid–base complex-like intermediate  $I_{[4+2]-[2+2]_{\text{CN}}}$  (**3a**) is found, in which the N atom acts as a Lewis base and the surface as a Lewis acid. The  $[4+2]$  and  $[2+2]_{\text{CN}}$  reaction mechanisms share the same intermediate,  $I_{[4+2]-[2+2]_{\text{CN}}}$ .

Surface isomerization reactions among possible surface products appear to be very unlikely due to the very large (~40 kcal/mol) activation barriers.

Consequently, the theoretical results presented here strongly suggest that there exists competition between the reaction channels leading to the  $[4+2]$  and  $[2+2]_{\text{CN}}$  products. So it is expected that both the  $[4+2]$  and  $[2+2]_{\text{CN}}$  products are formed

in the initial stages of these reactions and that they are not subjected to subsequent surface isomerization reactions. Therefore, it is concluded that the overall surface reactions of acrylonitrile with Si(100)-2×1 are controlled by kinetics, rather than by thermodynamics, as was found for homonuclear dienes.<sup>10</sup>

The foregoing conclusions suggest the need for a reinterpretation of the recent experiments.<sup>12</sup> The conclusion of the earlier study was primarily based on the absence of  $\nu(\text{C}\equiv\text{N})$  at 2245 cm<sup>-1</sup> and the appearance of  $\nu(\text{C}=\text{N})$  at 1669 cm<sup>-1</sup>, and on the preference for  $[2+2]_{\text{CN}}$  predicted by DFT calculations. However, the appearance of  $\nu(\text{C}=\text{N})$  at 1669 cm<sup>-1</sup> alone cannot rule out the existence of the  $[4+2]$  product. In fact, the experimental facts are also consistent with the existence of the  $[4+2]$  product since the  $[4+2]$  product also has a C=N double bond. Since the intensity of the C=N stretch vibration and the frequency of the cumulene structure (C=C=N) may be somewhat different from the normal C=N stretch, a more detailed vibrational analysis may be able to distinguish these two. In addition, the earlier DFT calculations appear to be in error, based on the exhaustive calculations reported here.

While single-configurational methods may be useful for studying the relative energies of the products, they are not appropriate to study the entire potential energy surface of dissociation/adsorption reactions. This is due to the highly multi-configurational nature of the reactants, as well as some of the intermediates and transition states, necessitating the use of multi-configurational descriptions to obtain reliable kinetic predictions.

It is clear from the current study that, to improve the surface selectivity toward a particular product, one must be able to control the kinetics. We are in the process of studying additional surface reactions to determine the generality of this conclusion.

**Acknowledgment.** This work was supported by grant No. R05-2002-000131-0 to C.H.C. from the Basic Research Program of the Korea Science & Engineering Foundation, and by grant No. F49620-99-1-0063 to M.S.G. from the U.S. Air Force Office of Scientific Research.

**Supporting Information Available:** Tables of geometric data (PDF). This material is available free of charge via the Internet at <http://pubs.acs.org>.

JA020147L